Title

Using Tumor Explants for Imaging Mass Spectrometry Visualization of Unlabeled Peptides and Small Molecules

Journal

ACS Medicinal Chemistry Letters, 9(7)

ISSN

1948-5875

Authors

David, Brian P
Dubrovskyi, Oleksii
Speltz, Thomas E
et al.

Publication Date

2018-07-12

DOI

10.1021/acsmedchemlett.8b00091

Peer reviewed

ACS Medicinal Chemistry Letters

Technology Note

Cite This: ACS Med. Chem. Lett. 2018, 9, 768−772

Using Tumor Explants for Imaging Mass Spectrometry Visualization of Unlabeled Peptides and Small Molecules

Brian P. David,[†] Oleksii Dubrovskyi,[‡] Thomas E. Speltz,[†] Jeremy J. Wolff,[§] Jonna Frasor,[‡] Laura M. Sanchez,[†] and Terry W. Moore*[,†]

[†]Department of Medicinal Chemistry and Pharmacognosy and UI Cancer Center, University of Illinois at Chicago, 833 South Wood Street, Chicago, Illinois 60612, United States

[‡]Department of Physiology and Biophysics and UI Cancer Center, University of Illinois at Chicago, 835 South Wolcott, Chicago, Illinois 60623, United States

[§]Bruker Daltonics, 40 Manning Road, Billerica, Massachusetts 01821, United States

Supporting Information

ABSTRACT: Matrix assisted laser desorption ionization time-of-flight (MALDI-TOF) imaging mass spectrometry has emerged as a powerful, label-free technique to visualize penetration of small molecules *in vivo* and *in vitro*, including in 3D cell culture spheroids; however, some spheroids do not grow sufficiently large to provide enough area for imaging mass spectrometry. Here, we describe an *ex vivo* method for visualizing unlabeled peptides and small molecules in tumor explants, which can be divided into pieces of desired size, thus circumventing the size limitations of many spheroids. As proof-of-concept, a small molecule drug (4-hydroxytamoxifen), as well as a peptide drug (cyclosporin A) and peptide chemical probe, can be visualized after *in vitro* incubation with tumor explants so that this technique may provide a solution to robing cell penetration by unlabeled peptides.

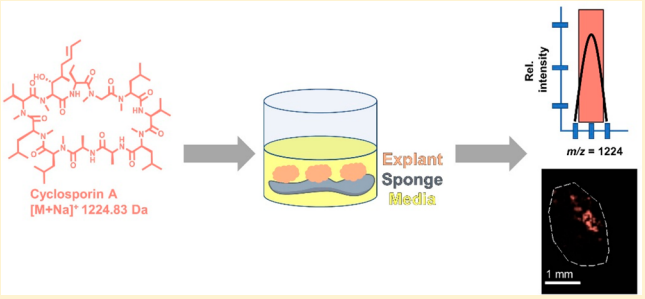

KEYWORDS: *Cancer, cell penetration, explants, MALDI-TOF, mass spectrometry*

Matrix assisted laser desorption ionization coupled to time-of-flight mass spectrometry (MALDI-TOF) has been used extensively for the rapid acquisition of mass-to-charge ratios (m/z) of samples cocrystallized in a matrix.[1] MALDI-TOF can be used in an imaging mode by collecting mass spectra at high spatial resolution across a biological sample.[2] Caprioli and co-workers were among the first to apply MALDI-TOF mass spectrometry to image tissue and create a localization map of endogenous peptides.[3] Because it relies only on the inherent m/z of an analyte, MALDI-TOF imaging mass spectrometry does not require the use of a chemical label for visualization, which presents an intriguing option to visualize the cellular uptake of small molecules and peptides. Beyond the initial reports, imaging mass spectrometry has been extended to include other milieus, including cell culture, tissue microarrays, organs, and model organisms, among others. Notably, Hummon and co-workers have developed a method for visualizing the permeability of irinotecan, a small molecule cancer drug, into 3D colon cancer spheroids using MALDI-TOF imaging mass spectrometry.[4−6]

Beyond colon cancer, there are a number of other cancer cell lines that have been used to generate spheroids;[7] however, depending on the cell line and method used to prepare spheroids, it can be difficult to obtain spheroids of uniform and/or large size.[8] For instance, while colon cancer spheroids can be grown to relatively large diameters (1000 μm), we could grow estrogen receptor-positive (ER+) breast cancer spheroids to diameters of only ca. 95 μm. The spatial resolution of imaging mass spectrometry is 10−100 μm, so that such small breast cancer spheroids would not generate enough raster spots from the MALDI-TOF imaging mass spectrometry to provide a complete spatial uptake map.[4] Given the myriad number of experimental procedures that exist for the formation of spheroids and the differences in sizes of spheroids generated from these procedures, there is an advantage in controlling the size of the sample to be imaged using MALDI.[7,9,10]

To address this shortcoming, we used explant cultures of breast tumors, which represent a powerful new approach to study drug response in xenograft tumors. Briefly, explants are pieces of a xenograft tumor that can be treated *ex vivo*. They are valuable research tools because they capture tumor heterogeneity and cell−cell interactions better than cell culture models or spheroid cultures.[11−14] An additional advantage of explants is that, because we could divide a xenograft into explants of a desired size, we could circumvent the size limitation of 3D spheroids. We saw an opportunity to treat

Received: February 21, 2018
Accepted: May 17, 2018
Published: May 17, 2018

DOI: 10.1021/acsmedchemlett.8b00091
ACS Med. Chem. Lett. 2018, 9, 768−772

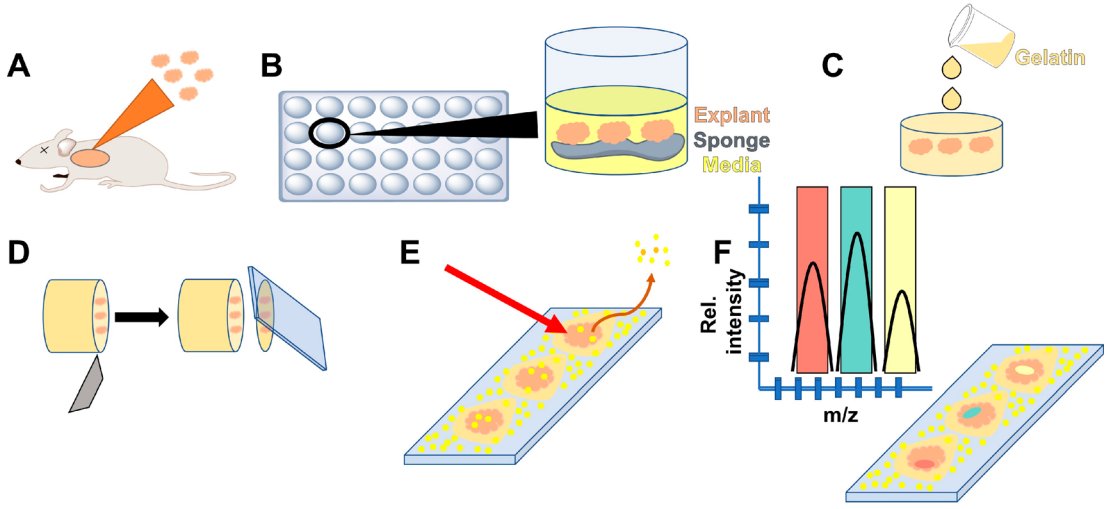

Figure 1. Workflow of explant-based imaging mass spectrometry. (A) Xenograft tumors are harvested from mammary glands of mice. (B) Tumors are trimmed, divided into explants of desired size, and treated. (C) Treated explants are embedded into gelatin. (D) Embedded explants are cryosectioned into 6−12 μm thick sections and thaw-mounted onto indium tin oxide slides. (E) MALDI matrix is applied, and the slide is inserted into the MALDI-TOF mass spectrometer, in which the laser is guided to hit a region of interest in the sample. (F) Once data are generated, peaks of interest can be extracted and viewed in the sample to generate an image.

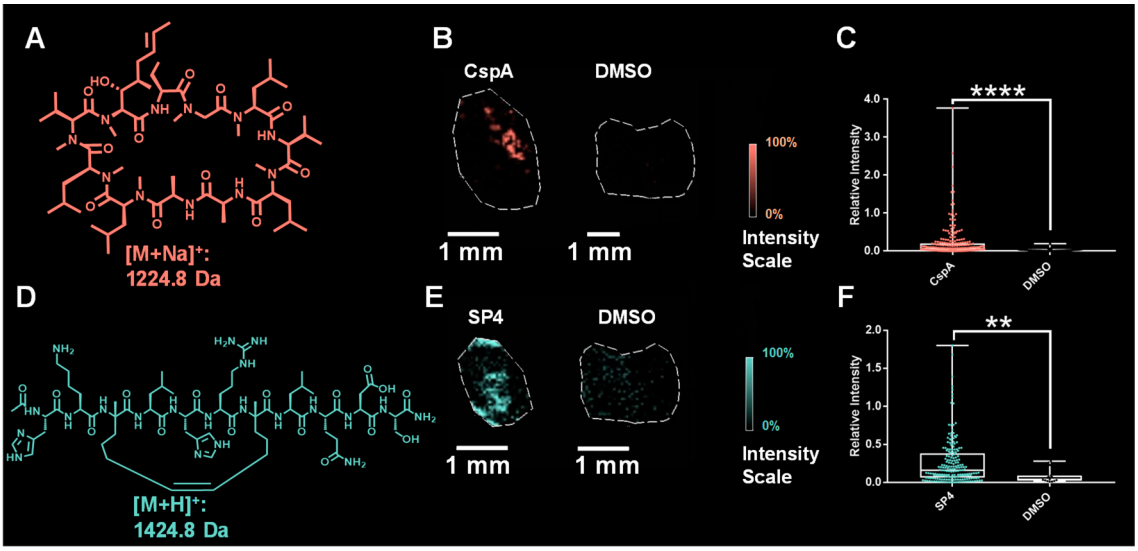

Figure 2. (A) Structure of macrocyclic peptide drug, cyclosporin A. (B) MALDI-TOF imaging mass spectrometry color image of CspA (m/z 1224.7 ± 0.2 Da and subsequent isotopic peaks $[M + Na]^+$, data were normalized between 2−28% to reflect 0−100% intensity scale) mass peaks detected in explant compared to explant treated with DMSO (scale bar = 1 mm). (C) Box-and-whiskers plot of m/z signal 1224.8 in CspA-treated explant and DMSO-treated explant. (D) Structure of α-helical peptide, SRC2-SP4. (E) MALDI imaging mass spectrometry color image of SRC2-SP4 (m/z 1424.9 ± 0.2 Da and subsequent isotopic peaks $[M + H]^+$, data were normalized between 10−60% to reflect 0−100% intensity scale) mass peaks detected in explant compared to explant treated with DMSO (scale bar = 1 mm). (F) Box-and-whiskers plots of m/z signal 1424.8 in SRC2-SP4-treated explant and DMSO-treated explant. ****$p < 0.0001$; **$p < 0.01$.

explants with different drugs and chemical probes and then to visualize the uptake of these molecules using imaging mass spectrometry.

We were particularly interested in using explant-based imaging mass spectrometry to visualize uptake of peptides. Penetration of cells and tissues by peptides is of considerable interest, but most assays for determining uptake rely upon detection of a chemical label. Although a state-of-the-art assay relies upon only a chloroalkyl group as a label in a Halo-Tag assay,[15] two common methods for visualizing and quantifying peptide uptake are high-resolution fluorescence microscopy and flow cytometry, both of which require a fluorophore label.[15−18] One assay has used both techniques in a high-throughput manner to quantify the uptake of an array of peptides.[18] Fluorophore-modified peptides may not have the same properties as their unlabeled counterparts. For instance, tagging a peptide with a fluorophore can affect various properties, including cellular penetration,[19] avidity,[20] distribution,[21] and subcellular localization;[22] thus, because of its ability to monitor unmodified species, imaging mass spectrometry may provide an advantage when imaging peptides, in particular.

The overall workflow of our method is shown in Figure 1. Breast tumor xenografts from the ER+ MCF-7 cell line are grown in female athymic nude (nu/nu) mice. Tumors are harvested and cut to ∼1 mm^3, a sample size large enough to collect a sufficient amount of data for interpretation. Pieces are

DOI: 10.1021/acsmedchemlett.8b00091
ACS Med. Chem. Lett. 2018, 9, 768−772

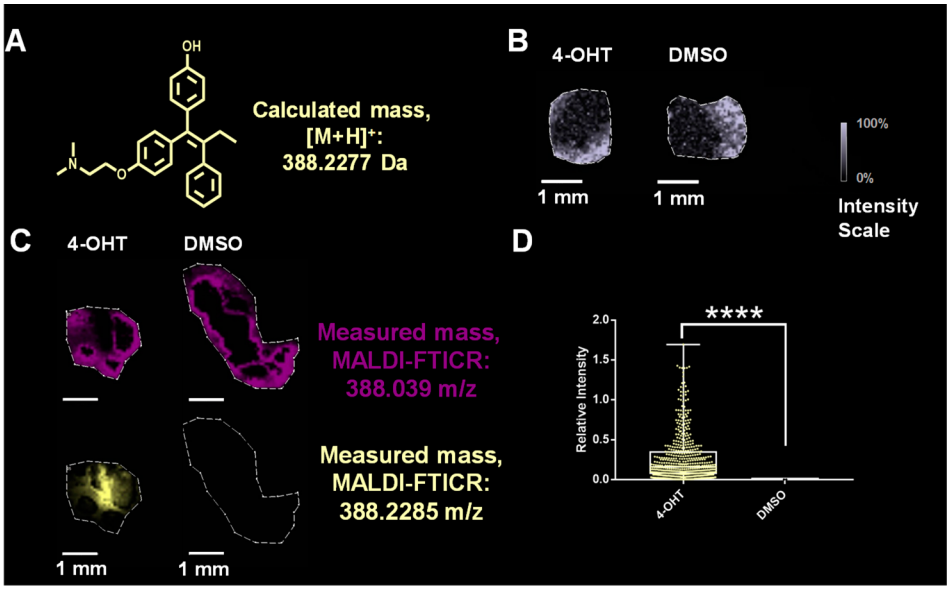

Figure 3. (A) Structure of the selective estrogen receptor modulator 4-OHT. (B) MALDI-TOF image showing the extracted mass signal of 4-OHT (388 m/z ± 0.2 Da and subsequent isotopic peaks, $[M + H]^+$, data were normalized between 2−28% to reflect 0−100% intensity scale) from a MALDI-TOF (scale bar = 1 mm). (C) High-resolution images acquired on MALDI-FT-ICR of samples treated for 24 h with 1 μM 4-OHT (scale bar = 1 mm). When resolved, a difference can be seen from the extracted, localized mass of 388.039 m/z (±0.005 Da) (top) and the extracted, localized mass of 388.2285 m/z (±0.005 Da) (bottom), the latter of which corresponds to the exact mass of 4-OHT (m/z = 388.2277). (D) Statistical analysis of m/z signal of 388.2285 in 4-OHT treated explant and DMSO treated explant. ****p < 0.0001.

cultured as explants and then treated with various drugs *ex vivo*. After treatment, samples are prepared, cryosectioned, and analyzed using the label-free MALDI-TOF imaging mass spectrometry technique.

Tumor explants of ∼1 mm^3 were supported on a gelatin sponge in culture and treated for 24 h with varying concentrations of probe and/or drug molecule. Treated explants were embedded in gelatin and cryosectioned between 6 and 12 μm thickness. Gelatin sections were thaw-mounted onto indium tin oxide slides (Figure 1D). The slides were stored in a desiccator until matrix was applied using an automated MALDI matrix applicator. The matrix chosen for these experiments was a 50:50 mixture of 2,5-dihydroxybenzoic acid (DHB) and α-cyano-4-hydroxycinnamic acid (CHCA), which was dissolved in acetone to make a 10% solution. DHB and CHCA are generally chosen for small molecules and other analytes of low mass (mass < 5000 Da). Mass spectrometry imaging analysis was then performed with a Bruker Autoflex speed LRF MALDI-TOF spectrometer (Figure 1E,F). To model the explant system with a known peptide drug, we chose cyclosporin A (CspA, Figure 2A) as a proof-of-concept. Cyclosporin A is an orally bioavailable macrocyclic peptide immunosuppressant given for a number of diseases, including rheumatoid arthritis and dry eyes.[23] It is known that 5 μM cyclosporin A can inhibit glucosylceramide formation in 2D MCF-7 cell culture, so that there is good evidence for its uptake by MCF-7 cells.[24] With this in mind, MCF-7 tumor explants were treated with 5 μM CspA for 24 h. Compared to the explants treated with DMSO vehicle, the signal intensities for the sodium adduct of CspA are significantly different (****p < 0.0001) (Figure 2C) and are within the explant, signaling that CspA has been taken up and internalized by the explants. The sodium adduct peak is shown for analysis because its intensity was higher than the $[M + H]^+$ peak in the spectrum of CspA (Figure S1), correlating with the dried droplet method of analyzing CspA by MALDI-TOF, indicating it more readily ionizes via MALDI than the $[M + H]^+$. When looking at additional thaw-mounted sections of explants treated with CspA, serial sectioning shows that CspA has been taken up by other layers of the same explant (Figure S2).

Encouraged by our results with cyclosporin A, we treated MCF-7 explants with one of our previously reported stapled peptides, SRC2-SP4,[25] which is an inhibitor of the estrogen receptor/steroid receptor coactivator interaction. Xenograft explants were treated with 25 μM SRC2-SP4, similar to concentrations used in previous work.[26] Similar to CspA, the intensity of the peptide inside the explants is significantly higher (**p = 0.0022) (Figure 2F) than the same peak extracted in the DMSO vehicle-treated explants (Figure 2B). While we have not carried out concentration−response experiments, we speculate that an increase in concentration should lead to an increase in signal intensity; however, in this case, concentrations higher than 25 μM may not be desirable. Again, the spectra obtained from imaging mass spectrometry match the data generated from a stock solution of pure peptide with the dried droplet method (Figure S1). Because of the relatively poor ionization of SRC2-SP4, the signal-to-noise is lower than for other analytes (Figure 2E), which demonstrates one of the shortcomings of this method: the signal is dependent upon the ionization efficiency of the analyte.

Tamoxifen is a known selective estrogen receptor modulator, and its bioactive metabolite 4-hydroxytamoxifen (4-OHT) has mixed agonist/antagonist effects on the estrogen receptor.[27] Similarly to CspA and SP4, explants were treated with 1 μM 4-hydroxytamoxifen, a commonly used dose,[28] for 24 h. Initial MALDI IMS experiments using a Bruker Autoflex speed LRF MALDI-TOF instrument demonstrated that the resolving power of this instrument was insufficient to separate $[M + H]^+$ signal of 4-OHT from an interfering ion of 388 m/z seen in the DMSO-treated explant (Figure 3C). When analyzed by a MALDI-FT-ICR instrument (Bruker), the peak seen at 388 m/z can be resolved into two peaks, one of which is within 2.06

DOI: 10.1021/acsmedchemlett.8b00091
ACS Med. Chem. Lett. 2018, 9, 768−772

ppm of the theoretical mass of the expected $[M + H]^+$ peak of 4-OHT (388.2277 m/z) (Figure 3C). As seen in Figure 3C, the 388.2285 m/z peak is extracted and only viewed in the explants treated with 4-hydroxytamoxifen (****$p < 0.0001$). The other signal, 388.039, is seen in explants treated with either 4-OHT or DMSO (Figure 3C). These data suggest that the explant model for visualization of small molecules and other probes is viable. It also shows that high-resolution instruments can resolve signals that have similar molecular weights to the mass or mass range of interest. These data are in good agreement with a previous study in which tamoxifen was detected by mass spectrometry after being sprayed onto tumor sections.[29]

In conclusion, we have developed an imaging mass spectrometry model for monitoring the uptake of macrocyclic peptides/probes and small molecules *ex vivo* in tumor explants. The strength of this method lies in the ability to divide tumor explants into a desired size, which bypasses the current size limitations of some small-growing spheroids, such as those derived from MCF-7. This technique could potentially be useful for other cancer cell lines that do not form uniformly sized spheroids. Future work may apply this approach to explants derived from patient-derived xenografts or from other tumor types. Additionally, these studies could provide a useful approach to understanding the effect of tumor heterogeneity on drug uptake, efflux, or efficacy.

■ ASSOCIATED CONTENT

Supporting Information

The Supporting Information is available free of charge on the ACS Publications website at DOI: 10.1021/acsmedchemlett.8b00091.

Methods, care of explants, and additional spectral data (PDF)

■ AUTHOR INFORMATION

Corresponding Author

*E-mail: twmoore@uic.edu.

ORCID

Brian P. David: 0000-0001-5328-5394
Thomas E. Speltz: 0000-0001-9551-9080
Laura M. Sanchez: 0000-0001-9223-7977
Terry W. Moore: 0000-0002-5410-306X

Author Contributions

The manuscript was written through contributions of all authors. All authors have given approval to the final version of the manuscript.

Funding

This work was funded by the University of Illinois Cancer Center (to T.W.M.), Chicago Biomedical Consortium with support from the Searle Funds at The Chicago Community Trust (to T.W.M., L.M.S., and J.F.), Grant Number K12HD055892 from the National Institute of Child Health and Human Development (NICHD) and the National Institutes of Health Office of Research on Women's Health (ORWH) (to L.M.S.), and by UIC Startup funds (to L.M.S.). T.E.S. is funded by training grant T32 AT007533, sponsored by the Office of the NIH Director and the National Center for Complementary and Integrative Health.

Notes

The authors declare no competing financial interest.

■ ACKNOWLEDGMENTS

We thank Gabe LaBonia and Dr. Amanda Hummon (University of Notre Dame) for providing training with the MALDI-TOF imaging mass spectrometry methodology, Rami Hayajneh (Research Resources Center, UIC) for providing assistance with cryosectioning, and Dr. Michael Federle (UIC) for providing a sample of cyclosporin A.

■ ABBREVIATIONS

4-OHT, 4-hydroxytamoxifen; CHCA, α-cyano-4-hydroxycinnamic acid; CspA, cyclosporin A; DHB, 2,5-dihydroxybenzoic acid; DMSO, dimethyl sulfoxide; ER+, estrogen receptor positive; MALDI-TOF, matrix assisted laser desorption ionization time-of-flight; MALDI-FT-ICR, matrix assisted laser desorption ionization Fourier transfer ion cyclotron resonance; SRC2-SP4, steroid receptor coactivator 2 stapled peptide 4

■ REFERENCES

(1) Vorm, O; Roepstorff, P.; Mann, M. Imrpoved Resolution and Very High Sensitivity in MALDI TOF of Matrix Surfaces Made by Fast Evaporation. *Anal. Chem.* **1994**, *66* (19), 3281−3287.

(2) Cole, L. M.; Clench, M. R. Mass spectrometry imaging for the proteomic study of clinical tissue. *Proteomics: Clin. Appl.* **2015**, *9* (3−4), 335−41.

(3) Caprioli, R. M.; Farmer, T. B.; Gile, J. Molecular imaging of biological samples: localization of peptides and proteins using MALDI-TOF MS. *Anal. Chem.* **1997**, *69* (23), 4751−60.

(4) Ahlf Wheatcraft, D. R.; Liu, X.; Hummon, A. B. Sample preparation strategies for mass spectrometry imaging of 3D cell culture models. *J. Visualized Exp.* **2014**, No. 94, e52313.

(5) Liu, X.; Hummon, A. B. Mass spectrometry imaging of therapeutics from animal models to three-dimensional cell cultures. *Anal. Chem.* **2015**, *87* (19), 9508−19.

(6) Liu, X.; Weaver, E. M.; Hummon, A. B. Evaluation of therapeutics in three-dimensional cell culture systems by MALDI imaging mass spectrometry. *Anal. Chem.* **2013**, *85* (13), 6295−302.

(7) Nath, S.; Devi, G. R. Three-dimensional culture systems in cancer research: Focus on tumor spheroid model. *Pharmacol. Ther.* **2016**, *163*, 94−108.

(8) Achilli, T. M.; Meyer, J.; Morgan, J. R. Advances in the formation, use and understanding of multi-cellular spheroids. *Expert Opin. Biol. Ther.* **2012**, *12* (10), 1347−60.

(9) Vinci, M.; Gowan, S.; Boxall, F.; Patterson, L.; Zimmermann, M.; Court, W.; Lomas, C.; Mendiola, M.; Hardisson, D.; Eccles, S. A. Advances in establishment and analysis of three-dimensional tumor spheroid-based functional assays for target validation and drug evaluation. *BMC Biol.* **2012**, *10*, 29.

(10) Zanoni, M.; Piccinini, F.; Arienti, C.; Zamagni, A.; Santi, S.; Polico, R.; Bevilacqua, A.; Tesei, A. 3D tumor spheroid models for in vitro therapeutic screening: a systematic approach to enhance the biological relevance of data obtained. *Sci. Rep.* **2016**, *6*, 19103.

(11) Majumder, B.; Baraneedharan, U.; Thiyagarajan, S.; Radhakrishnan, P.; Narasimhan, H.; Dhandapani, M.; Brijwani, N.; Pinto, D. D.; Prasath, A.; Shanthappa, B. U.; Thayakumar, A.; Surendran, R.; Babu, G. K.; Shenoy, A. M.; Kuriakose, M. A.; Bergthold, G.; Horowitz, P.; Loda, M.; Beroukhim, R.; Agarwal, S.; Sengupta, S.; Sundaram, M.; Majumder, P. K. Predicting clinical response to anticancer drugs using an ex vivo platform that captures tumour heterogeneity. *Nat. Commun.* **2015**, *6*, 6169.

(12) Davies, E. J.; Dong, M.; Gutekunst, M.; Narhi, K.; van Zoggel, H. J.; Blom, S.; Nagaraj, A.; Metsalu, T.; Oswald, E.; Erkens-Schulze, S.; Delgado San Martin, J. A.; Turkki, R.; Wedge, S. R.; af Hallstrom, T. M.; Schueler, J.; van Weerden, W. M.; Verschuren, E. W.; Barry, S. T.; van der Kuip, H.; Hickman, J. A. Capturing complex tumour biology in vitro: histological and molecular characterisation of precision cut slices. *Sci. Rep.* **2015**, *5*, 17187.

DOI: 10.1021/acsmedchemlett.8b00091
ACS Med. Chem. Lett. 2018, 9, 768−772

(13) van der Kuip, H.; Murdter, T. E.; Sonnenberg, M.; McClellan, M.; Gutzeit, S.; Gerteis, A.; Simon, W.; Fritz, P.; Aulitzky, W. E. Short term culture of breast cancer tissues to study the activity of the anticancer drug taxol in an intact tumor environment. *BMC Cancer* **2006**, *6*, 86.
(14) Hickman, J. A.; Graeser, R.; de Hoogt, R.; Vidic, S.; Brito, C.; Gutekunst, M.; van der Kuip, H. Three-dimensional models of cancer for pharmacology and cancer cell biology: capturing tumor complexity in vitro/ex vivo. *Biotechnol. J.* **2014**, *9* (9), 1115−28.
(15) Peraro, L.; Zou, Z.; Makwana, K. M.; Cummings, A. E.; Ball, H. L.; Yu, H.; Lin, Y. S.; Levine, B.; Kritzer, J. A. Diversity-Oriented Stapling Yields Intrinsically Cell-Penetrant Inducers of Autophagy. *J. Am. Chem. Soc.* **2017**, *139* (23), 7792−7802.
(16) Rodrigues, M.; de la Torre, B. G.; Andreu, D.; Santos, N. C. Kinetic uptake profiles of cell penetrating peptides in lymphocytes and monocytes. *Biochim. Biophys. Acta, Gen. Subj.* **2013**, *1830* (10), 4554−63.
(17) Fischer, R.; Kohler, K.; Fotin-Mleczek, M.; Brock, R. A stepwise dissection of the intracellular fate of cationic cell-penetrating peptides. *J. Biol. Chem.* **2004**, *279* (13), 12625−35.
(18) Chu, Q.; Hilinski, G. J.; Kim, Y.-W.; Grossmann, T. N.; Yeh, J. T.-H.; Verdine, G. L.; Moellering, R. E. Towards understanding cell penetration by stapled peptides. *MedChemComm* **2015**, *6*, 111.
(19) Fischer, R.; Waizenegger, T.; Kohler, K.; Brock, R. A quantitative validation of fluorophore-labelled cell-permeable peptide conjugates: fluorophore and cargo dependence of import. *Biochim. Biophys. Acta, Biomembr.* **2002**, *1564* (2), 365−74.
(20) Vira, S.; Mekhedov, E.; Humphrey, G.; Blank, P. S. Fluorescent-labeled antibodies: Balancing functionality and degree of labeling. *Anal. Biochem.* **2010**, *402* (2), 146−50.
(21) Sanchez, L. M.; Knudsen, G. M.; Helbig, C.; De Muylder, G.; Mascuch, S. M.; Mackey, Z. B.; Gerwick, L.; Clayton, C.; McKerrow, J. H.; Linington, R. G. Examination of the mode of action of the almiramide family of natural products against the kinetoplastid parasite Trypanosoma brucei. *J. Nat. Prod.* **2013**, *76* (4), 630−41.
(22) Puckett, C. A.; Barton, J. K. Fluorescein redirects a ruthenium-octaarginine conjugate to the nucleus. *J. Am. Chem. Soc.* **2009**, *131* (25), 8738−9.
(23) Donnenfeld, E.; Pflugfelder, S. C. Topical ophthalmic cyclosporine: pharmacology and clinical uses. *Surv. Ophthalmol.* **2009**, *54* (3), 321−38.
(24) Lavie, Y.; Cao, H.; Volner, A.; Lucci, A.; Han, T. Y.; Geffen, V.; Giuliano, A. E.; Cabot, M. C. Agents that reverse multidrug resistance, tamoxifen, verapamil, and cyclosporin A, block glycosphingolipid metabolism by inhibiting ceramide glycosylation in human cancer cells. *J. Biol. Chem.* **1997**, *272* (3), 1682−7.
(25) Speltz, T. E.; Fanning, S. W.; Mayne, C. G.; Fowler, C.; Tajkhorshid, E.; Greene, G. L.; Moore, T. W. Stapled Peptides with gamma-Methylated Hydrocarbon Chains for the Estrogen Receptor/Coactivator Interaction. *Angew. Chem., Int. Ed.* **2016**, *55* (13), 4252−5.
(26) Speltz, T. E.; Danes, J. M.; Stender, J. D.; Frasor, J.; Moore, T. W. A Cell-Permeable Stapled Peptide Inhibitor of the Estrogen Receptor/Coactivator Interaction. *ACS Chem. Biol.* **2018**, *13* (3), 676−684.
(27) Jordan, V. C. Tamoxifen: a most unlikely pioneering medicine. *Nat. Rev. Drug Discovery* **2003**, *2* (3), 205−13.
(28) Huang, L.; Zhao, S.; Frasor, J. M.; Dai, Y. An integrated bioinformatics approach identifies elevated cyclin E2 expression and E2F activity as distinct features of tamoxifen resistant breast tumors. *PLoS One* **2011**, *6* (7), e22274.
(29) Vegvari, A.; Shavkunov, A. S.; Fehniger, T. E.; Grabau, D.; Nimeus, E.; Marko-Varga, G. Localization of tamoxifen in human breast cancer tumors by MALDI mass spectrometry imaging. *Clin Transl Med.* **2016**, *5* (1), 10.

DOI: 10.1021/acsmedchemlett.8b00091
ACS Med. Chem. Lett. 2018, 9, 768−772